

Direct evidence for efficient ultrafast charge separation in epitaxial WS₂/graphene heterostructures

Sven Aeschlimann, Antonio Rossi, Mariana Chávez-Cervantes, Razvan Krause, Benito Arnoldi, Benjamin Stadtmüller, Martin Aeschlimann, Stiven Forti, Filippo Fabbri, Camilla Coletti, Isabella Gierz

Angaben zur Veröffentlichung / Publication details:

Aeschlimann, Sven, Antonio Rossi, Mariana Chávez-Cervantes, Razvan Krause, Benito Arnoldi, Benjamin Stadtmüller, Martin Aeschlimann, et al. 2020. "Direct evidence for efficient ultrafast charge separation in epitaxial WS₂/graphene heterostructures." *Science Advances* 6 (20): eaay0761.
<https://doi.org/10.1126/sciadv.aay0761>.

PHYSICS

Direct evidence for efficient ultrafast charge separation in epitaxial WS₂/graphene heterostructures

Sven Aeschlimann^{1,2*}, Antonio Rossi^{3,4}, Mariana Chávez-Cervantes¹, Razvan Krause^{1,2}, Benito Arnoldi⁵, Benjamin Stadtmüller⁵, Martin Aeschlimann⁵, Stiven Forti³, Filippo Fabbri^{3,4,6}, Camilla Coletti^{3,6}, Isabella Gierz^{1,2*}

We use time- and angle-resolved photoemission spectroscopy (tr-ARPES) to investigate ultrafast charge transfer in an epitaxial heterostructure made of monolayer WS₂ and graphene. This heterostructure combines the benefits of a direct-gap semiconductor with strong spin-orbit coupling and strong light-matter interaction with those of a semimetal hosting massless carriers with extremely high mobility and long spin lifetimes. We find that, after photoexcitation at resonance to the A-exciton in WS₂, the photoexcited holes rapidly transfer into the graphene layer while the photoexcited electrons remain in the WS₂ layer. The resulting charge-separated transient state is found to have a lifetime of ~1 ps. We attribute our findings to differences in scattering phase space caused by the relative alignment of WS₂ and graphene bands as revealed by high-resolution ARPES. In combination with spin-selective optical excitation, the investigated WS₂/graphene heterostructure might provide a platform for efficient optical spin injection into graphene.

INTRODUCTION

The availability of many different two-dimensional materials has opened up the possibility to create novel ultimately thin heterostructures with completely new functionalities based on tailored dielectric screening and various proximity-induced effects (1–3). Proof-of-principle devices for future applications in the field of electronics and optoelectronics have been realized (4–6).

Here, we focus on epitaxial van der Waals heterostructures consisting of monolayer WS₂, a direct-gap semiconductor with strong spin-orbit coupling and a sizable spin splitting of the band structure due to broken inversion symmetry (7), and monolayer graphene, a semimetal with conical band structure and extremely high carrier mobility (8), grown on hydrogen-terminated SiC(0001). First indications for ultrafast charge transfer (9–15) and proximity-induced spin-orbit coupling effects (16–18) make WS₂/graphene and similar heterostructures promising candidates for future optoelectronic (19) and optospintronic (20) applications.

We set out to reveal the relaxation pathways of photogenerated electron-hole pairs in WS₂/graphene with time- and angle-resolved photoemission spectroscopy (tr-ARPES). For that purpose, we excite the heterostructure with 2-eV pump pulses resonant to the A-exciton in WS₂ (21, 12) and eject photoelectrons with a second time-delayed probe pulse at 26-eV photon energy. We determine kinetic energy and emission angle of the photoelectrons with a hemispherical analyzer as a function of pump-probe delay to get access to the momentum-, energy-, and time-resolved carrier dynamics. The energy and time resolution is 240 meV and 200 fs, respectively.

¹Max Planck Institute for the Structure and Dynamics of Matter, Center for Free Electron Laser Science, Luruper Chaussee 149, 22761 Hamburg, Germany. ²University of Regensburg, Institute for Experimental and Applied Physics, Universitätsstr. 31, 93053 Regensburg, Germany. ³Center for Nanotechnology Innovation at NEST, Istituto Italiano di Tecnologia, Piazza S. Silvestro, 12, 56124 Pisa, Italy. ⁴NEST, Istituto Nanoscienze, CNR and Scuola Normale Superiore, Piazza S. Silvestro, 12, 56124 Pisa, Italy. ⁵University of Kaiserslautern, Department of Physics and Research Center OPTIMAS, Erwin Schrödinger Str. 46, 67663 Kaiserslautern, Germany. ⁶Graphene Labs, Istituto Italiano di Tecnologia, Via Morego 30, 16163 Genova, Italy.

*Corresponding author. Email: sven.aeschlimann@gmx.de (S.A.); isabella.gierz@ur.de (I.G.)

Our results provide direct evidence for ultrafast charge transfer between the epitaxially aligned layers, confirming first indications based on all-optical techniques in similar manually assembled heterostructures with arbitrary azimuthal alignment of the layers (9–15). In addition, we show that this charge transfer is highly asymmetric. Our measurements reveal a previously unobserved charge-separated transient state with photoexcited electrons and holes located in the WS₂ and graphene layer, respectively, that lives for ~1 ps. We interpret our findings in terms of differences in scattering phase space for electron and hole transfer caused by the relative alignment of WS₂ and graphene bands as revealed by high-resolution ARPES. Combined with spin- and valley-selective optical excitation (22–25) WS₂/graphene heterostructures might provide a new platform for efficient ultrafast optical spin injection into graphene.

RESULTS

Figure 1A shows a high-resolution ARPES measurement obtained with a helium lamp of the band structure along the Γ K-direction of the epitaxial WS₂/graphene heterostructure. The Dirac cone is found to be hole-doped with the Dirac point located ~0.3 eV above the equilibrium chemical potential. The top of the spin-split WS₂ valence band is found to be ~1.2 eV below the equilibrium chemical potential.

Figure 1B shows a tr-ARPES snapshot of the band structure close to the WS₂ and graphene K-points measured with 100-fs extreme ultraviolet pulses at 26-eV photon energy at negative pump-probe delay before the arrival of the pump pulse. Here, the spin splitting is not resolved because of sample degradation and the presence of the 2-eV pump pulse that causes space charge broadening of the spectral features. Figure 1C shows the pump-induced changes of the photocurrent with respect to Fig. 1B at a pump-probe delay of 200 fs where the pump-probe signal reaches its maximum. Red and blue colors indicate gain and loss of photoelectrons, respectively.

To analyze this rich dynamics in more detail, we first determine the transient peak positions of the WS₂ valence band and the

Copyright © 2020
The Authors, some
rights reserved;
exclusive licensee
American Association
for the Advancement
of Science. No claim to
original U.S. Government
Works. Distributed
under a Creative
Commons Attribution
NonCommercial
License 4.0 (CC BY-NC).

Downloaded from https://www.science.org at Universitaetshilthek Augsburg on May 14, 2024

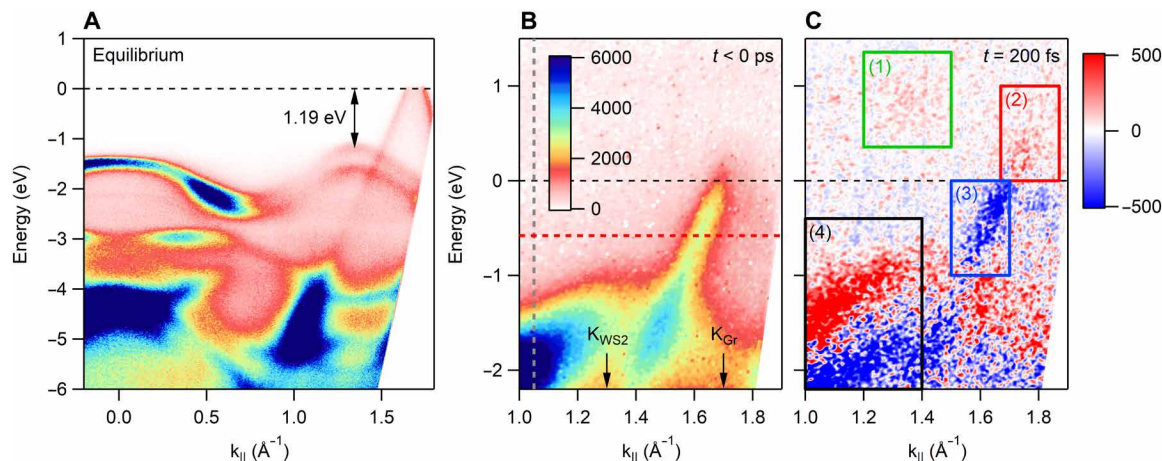


Fig. 1. Equilibrium band structure and photocarrier dynamics of WS₂/graphene heterostructure. (A) Equilibrium photocurrent measured along the ΓK -direction with an unpolarized helium lamp. (B) Photocurrent for negative pump-probe delay measured with p-polarized extreme ultraviolet pulses at 26-eV photon energy. Dashed gray and red lines mark the position of the line profiles used to extract the transient peak positions in Fig. 2. (C) Pump-induced changes of the photocurrent 200 fs after photoexcitation at a pump photon energy of 2 eV with a pump fluence of 2 mJ/cm². Gain and loss of photoelectrons are shown in red and blue, respectively. The boxes indicate the area of integration for the pump-probe traces displayed in Fig. 3.

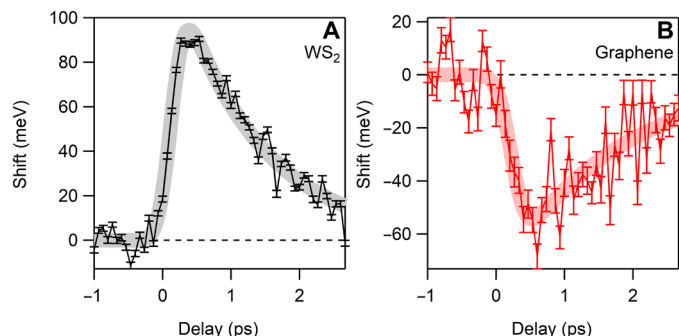


Fig. 2. Transient band shifts after photoexcitation. Change in peak position of the WS₂ valence band (A) and graphene π -band (B) as a function of pump-probe delay together with exponential fits (thick lines). The lifetime of the WS₂ shift in (A) is 1.2 ± 0.1 ps. The lifetime of the graphene shift in (B) is 1.7 ± 0.3 ps.

graphene π -band along the dashed lines in Fig. 1B as explained in detail in the Supplementary Materials. We find that the WS₂ valence band shifts up by 90 meV (Fig. 2A) and the graphene π -band shifts down by 50 meV (Fig. 2B). The exponential lifetime of these shifts is found to be 1.2 ± 0.1 ps for the valence band of WS₂ and 1.7 ± 0.3 ps for the graphene π -band. These peak shifts provide first evidence of a transient charging of the two layers, where additional positive (negative) charge increases (decreases) the binding energy of the electronic states. Note that the upshift of the WS₂ valence band is responsible for the prominent pump-probe signal in the area marked by the black box in Fig. 1C.

Next, we integrate the pump-probe signal over the areas indicated by the colored boxes in Fig. 1C and plot the resulting counts as a function of pump-probe delay in Fig. 3. Curve 1 in Fig. 3 shows the dynamics of the photoexcited carriers close to the bottom of the conduction band of the WS₂ layer with a lifetime of 1.1 ± 0.1 ps obtained from an exponential fit to the data (see the Supplementary Materials).

In curves 2 and 3 of Fig. 3, we show the pump-probe signal of the graphene π -band. We find that the gain of electrons above the equilib-

rium chemical potential (curve 2 in Fig. 3) has a much shorter lifetime (180 ± 20 fs) compared to the loss of electrons below the equilibrium chemical potential (1.8 ± 0.2 ps in curve 3 Fig. 3). Further, the initial gain of the photocurrent in curve 2 of Fig. 3 is found to turn into loss at $t = 400$ fs with a lifetime of ~ 2 ps. The asymmetry between gain and loss is found to be absent in the pump-probe signal of uncovered monolayer graphene (see fig. S5 in the Supplementary Materials), indicating that the asymmetry is a consequence of interlayer coupling in the WS₂/graphene heterostructure. The observation of a short-lived gain and long-lived loss above and below the equilibrium chemical potential, respectively, indicates that electrons are efficiently removed from the graphene layer upon photoexcitation of the heterostructure. As a result, the graphene layer becomes positively charged, which is consistent with the increase in binding energy of the π -band found in Fig. 2B. The downshift of the π -band removes the high-energy tail of the equilibrium Fermi-Dirac distribution from above the equilibrium chemical potential, which partly explains the change of sign of the pump-probe signal in curve 2 of Fig. 3. We will show below that this effect is further enhanced by the transient loss of electrons in the π -band.

This scenario is supported by the net pump-probe signal of the WS₂ valence band in curve 4 of Fig. 3. These data were obtained by integrating the counts over the area given by the black box in Fig. 1B that captures the electrons photoemitted from the valence band at all pump-probe delays. Within the experimental error bars, we find no indication for the presence of holes in the valence band of WS₂ for any pump-probe delay. This indicates that, after photoexcitation, these holes are rapidly refilled on a time scale short compared to our temporal resolution.

To provide final proof for our hypothesis of ultrafast charge separation in the WS₂/graphene heterostructure, we determine the number of holes transferred to the graphene layer as described in detail in the Supplementary Materials. In short, the transient electronic distribution of the π -band was fitted with a Fermi-Dirac distribution. The number of holes was then calculated from the resulting values for the transient chemical potential and electronic temperature. The result is shown in Fig. 4. We find that a total

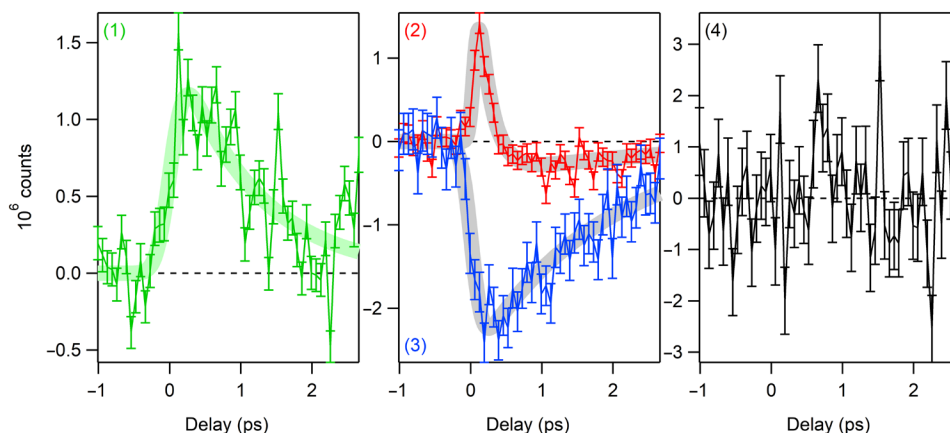


Fig. 3. Energy- and momentum-resolved carrier dynamics. Pump-probe traces as a function of delay obtained by integrating the photocurrent over the area indicated by the boxes in Fig. 1C. The thick lines are exponential fits to the data. Curve (1) Transient carrier population in the conduction band of WS₂. Curve (2) Pump-probe signal of the π -band of graphene above the equilibrium chemical potential. Curve (3) Pump-probe signal of the π -band of graphene below the equilibrium chemical potential. Curve (4) Net pump-probe signal in the valence band of WS₂. The lifetimes are found to be 1.2 ± 0.1 ps in (1), 180 ± 20 fs (gain) and ~ 2 ps (loss) in (2), and 1.8 ± 0.2 ps in (3).

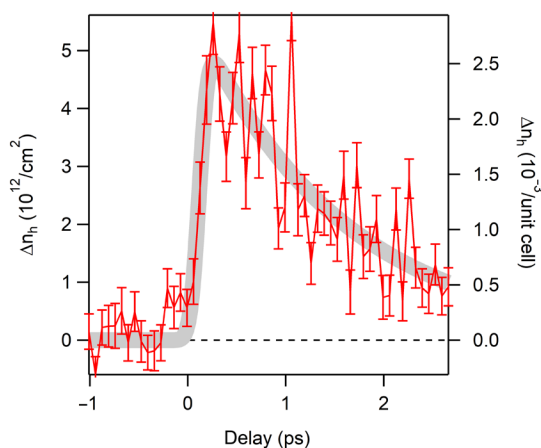


Fig. 4. Transient hole density in graphene layer. Change of the number of holes in the π -band as a function of pump-probe delay together with exponential fit yielding a lifetime of 1.5 ± 0.2 ps.

number of $\sim 5 \times 10^{12}$ holes/cm² are transferred from WS₂ to graphene with an exponential lifetime of 1.5 ± 0.2 ps.

DISCUSSION

From the findings in Figs. 2 to 4, the following microscopic picture for the ultrafast charge transfer in the WS₂/graphene heterostructure emerges (Fig. 5). Photoexcitation of the WS₂/graphene heterostructure at 2 eV dominantly populates the A-exciton in WS₂ (Fig. 5A). Additional electronic excitations across the Dirac point in graphene as well as between WS₂ and graphene bands are energetically possible but considerably less efficient. The photoexcited holes in the valence band of WS₂ are refilled by electrons originating from the graphene π -band on a time scale short compared to our temporal resolution (Fig. 5A). The photoexcited electrons in the conduction band of WS₂ have a lifetime of ~ 1 ps (Fig. 5B). However, it takes ~ 2 ps to refill the holes in the graphene π -band (Fig. 5B). This indicates that, aside from direct electron transfer between the WS₂ conduction band and the graphene π -band, additional relaxation pathways—possibly via defect states (26)—need to be considered to understand the full dynamics.

In the transient state, the photoexcited electrons reside in the conduction band of WS₂ while the photoexcited holes are located in the π -band of graphene (Fig. 5C). This means that the WS₂ layer is negatively charged and the graphene layer is positively charged. This accounts for the transient peak shifts (Fig. 2), the asymmetry of the graphene pump-probe signal (curves 2 and 3 of Fig. 3), the absence of holes in the valence band of WS₂ (curve 4 Fig. 3), as well as the additional holes in the graphene π -band (Fig. 4). The lifetime of this charge-separated state is ~ 1 ps (curve 1 Fig. 3).

Similar charge-separated transient states have been observed in related van der Waals heterostructures made out of two direct-gap semiconductors with type II band alignment and staggered bandgap (27–32). After photoexcitation, the electrons and holes were found to rapidly move to the bottom of the conduction band and to the top of the valence band, respectively, that are located in different layers of the heterostructure (27–32).

In the case of our WS₂/graphene heterostructure, the energetically most favorable location for both electrons and holes is at the Fermi level in the metallic graphene layer. Therefore, one would expect that both electrons and holes rapidly transfer to the graphene π -band. However, our measurements clearly show that hole transfer (< 200 fs) is much more efficient than electron transfer (~ 1 ps). We attribute this to the relative energetic alignment of the WS₂ and the graphene bands as revealed in Fig. 1A that offers a larger number of available final states for hole transfer compared to electron transfer as recently anticipated by (14, 15). In the present case, assuming a ~ 2 eV WS₂ bandgap, the graphene Dirac point and equilibrium chemical potential are located ~ 0.5 and ~ 0.2 eV above the middle of the WS₂ bandgap, respectively, breaking electron-hole symmetry. We find that the number of available final states for hole transfer is ~ 6 times larger than for electron transfer (see the Supplementary Materials), which is why hole transfer is expected to be faster than electron transfer.

A complete microscopic picture of the observed ultrafast asymmetric charge transfer should, however, also consider the overlap between the orbitals that constitute the A-exciton wave function in WS₂ and the graphene π -band, respectively, different electron-electron and electron-phonon scattering channels including the constraints imposed by momentum, energy, spin, and pseudospin conservation, the influence of plasma oscillations (33), as well as the role of a

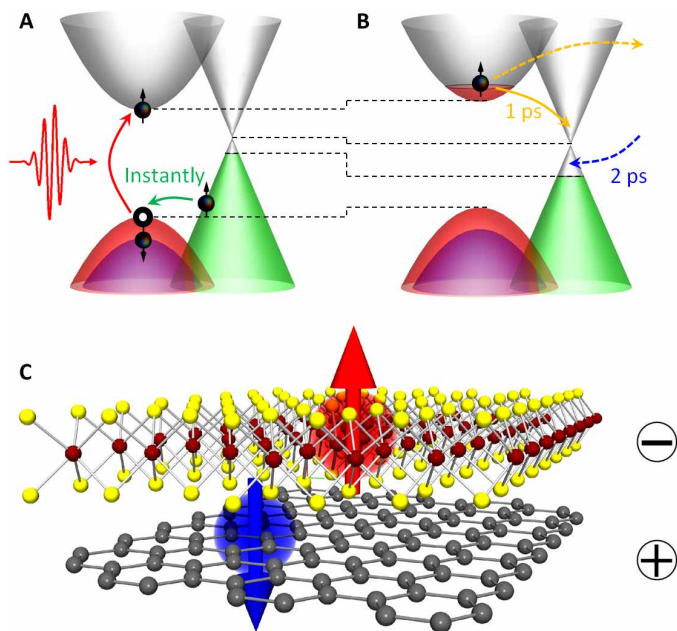


Fig. 5. Sketch of ultrafast charge transfer deduced from tr-ARPES data. (A) Photoexcitation at resonance to the WS₂ A-exciton at 2 eV injects electrons into the conduction band of WS₂. The corresponding holes in the valence band of WS₂ are instantly refilled by electrons from the graphene π -band. (B) The photoexcited carriers in the conduction band of WS₂ have a lifetime of ~ 1 ps. The holes in the graphene π -band live for ~ 2 ps, indicating the importance of additional scattering channels indicated by dashed arrows. Black dashed lines in (A) and (B) indicate band shifts and changes in chemical potential. (C) In the transient state, the WS₂ layer is negatively charged while the graphene layer is positively charged. For spin-selective excitation with circularly polarized light, the photoexcited electrons in WS₂ and the corresponding holes in graphene are expected to show opposite spin polarization.

possible displacive excitation of coherent phonon oscillations that might mediate the charge transfer (34, 35). Also, one might speculate whether the observed charge transfer state consists of charge transfer excitons or free electron-hole pairs (see the Supplementary Materials). Further theoretical investigations that go beyond the scope of the present paper are required to clarify these issues.

In summary, we have used tr-ARPES to study ultrafast interlayer charge transfer in an epitaxial WS₂/graphene heterostructure. We found that, when excited at resonance to the A-exciton of WS₂ at 2 eV, the photoexcited holes rapidly transfer into the graphene layer while the photoexcited electrons remain in the WS₂ layer. We attributed this to the fact that the number of available final states for hole transfer is larger than for electron transfer. The lifetime of the charge-separated transient state was found to be ~ 1 ps. In combination with spin-selective optical excitation using circularly polarized light (22–25), the observed ultrafast charge transfer might be accompanied by spin transfer. In this case, the investigated WS₂/graphene heterostructure might be used for efficient optical spin injection into graphene resulting in novel optospintronic devices.

MATERIALS AND METHODS

Sample fabrication

The graphene samples were grown on commercial semiconducting 6H-SiC(0001) wafers from SiCrystal GmbH. The N-doped wafers

were on-axis with a miscut below 0.5°. The SiC substrate was hydrogen-etched to remove scratches and obtain regular flat terraces. The clean and atomically flat Si-terminated surface was then graphitized by annealing the sample in Ar atmosphere at 1300°C for 8 min (36). This way, we obtained a single carbon layer where every third carbon atom formed a covalent bond to the SiC substrate (37). This layer was then turned into completely sp²-hybridized quasi free-standing hole-doped graphene via hydrogen intercalation (38). These samples are referred to as graphene/H-SiC(0001). The whole process was carried out in a commercial Black Magic growth chamber from Aixtron. The WS₂ growth was carried out in a standard hot-wall reactor by low-pressure chemical vapor deposition (39, 40) using WO₃ and S powders with a mass ratio of 1:100 as precursors. The WO₃ and S powders were kept at 900 and 200°C, respectively. The WO₃ powder was placed close to the substrate. Argon was used as carrier gas with a flow of 8 sccm. The pressure in the reactor was kept at 0.5 mbar. The samples were characterized with secondary electron microscopy, atomic force microscopy, Raman, and photoluminescence spectroscopy, as well as low-energy electron diffraction. These measurements revealed two different WS₂ single-crystalline domains where either the Γ K- or the Γ K'-direction is aligned with the Γ K-direction of the graphene layer. Domain side lengths varied between 300 and 700 nm, and the total WS₂ coverage was approximated to $\sim 40\%$, suitable for the ARPES analysis.

High-resolution ARPES

The static ARPES experiments were performed with a hemispherical analyzer (SPECS PHOIBOS 150) using a charge-coupled device-detector system for two-dimensional detection of electron energy and momentum. Unpolarized, monochromatic He I α radiation (21.2 eV) of a high-flux He discharge source (VG Scienta VUV5000) was used for all photoemission experiments. The energy and angular resolution in our experiments were better than 30 meV and 0.3° (corresponding to 0.01 \AA^{-1}), respectively. All experiments were conducted at room temperature. ARPES is an extremely surface-sensitive technique. To eject photoelectrons from both the WS₂ and the graphene layer, samples with an incomplete WS₂ coverage of $\sim 40\%$ were used.

Tr-ARPES

The tr-ARPES setup was based on a 1-kHz Titanium:Sapphire amplifier (Coherent Legend Elite Duo). 2 mJ of output power was used for high harmonics generation in argon. The resulting extreme ultraviolet light passed through a grating monochromator producing 100-fs probe pulses at 26-eV photon energy. 8 mJ of amplifier output power was sent into an optical parametric amplifier (HE-TOPAS from Light Conversion). The signal beam at 1-eV photon energy was frequency-doubled in a beta barium borate crystal to obtain the 2-eV pump pulses. The tr-ARPES measurements were performed with a hemispherical analyzer (SPECS PHOIBOS 100). The overall energy and temporal resolution was 240 meV and 200 fs, respectively.

SUPPLEMENTARY MATERIALS

Supplementary material for this article is available at <http://advances.sciencemag.org/cgi/content/full/6/20/eaay0761/DC1>

REFERENCES AND NOTES

1. A. K. Geim, I. V. Grigorieva, Van der Waals heterostructures. *Nature* **499**, 419–425 (2013).
2. K. S. Novoselov, A. Mishchenko, A. Carvalho, A. H. Castro Neto, 2D materials and van der Waals heterostructures. *Science* **353**, aac9439 (2016).

3. Y. Liu, N. O. Weiss, X. Duan, H.-C. Cheng, Y. Huang, X. Duan, Van der Waals heterostructures and devices. *Nat. Rev. Mater.* **1**, 16042 (2016).
4. T. Georgiou, R. Jalil, B. D. Belle, L. Britnell, R. V. Gorbachev, S. V. Morozov, Y.-J. Kim, A. Gholinia, S. J. Haigh, O. Makarovskiy, L. Eaves, L. A. Ponomarenko, A. K. Geim, K. S. Novoselov, A. Mishchenko, Vertical field-effect transistor based on graphene- WS_2 heterostructures for flexible and transparent electronics. *Nat. Nanotechnol.* **8**, 100–103 (2013).
5. F. H. L. Koppens, T. Mueller, P. Avouris, A. C. Ferrari, M. S. Vitiello, M. Polini, Photodetectors based on graphene, other two-dimensional materials and hybrid systems. *Nat. Nanotechnol.* **9**, 780–793 (2014).
6. Z. Li, C. Cheng, N. Dong, C. Romero, Q. Lu, J. Wang, J. R. V. de Aldana, Y. Tan, F. Chen, Q-switching of waveguide lasers based on graphene/ WS_2 van der Waals heterostructure. *Photonics Res.* **5**, 406–410 (2017).
7. Z. Y. Zhu, Y. C. Cheng, U. Schwingenschlögl, Giant spin-orbit-induced spin splitting in two-dimensional transition-metal dichalcogenide semiconductors. *Phys. Rev. B* **84**, 153402 (2011).
8. K. S. Novoselov, A. K. Geim, S. V. Morozov, D. Jiang, M. I. Katsnelson, I. V. Grigorieva, S. V. Dubonos, A. A. Firsov, Two-dimensional gas of massless Dirac fermions in graphene. *Nature* **438**, 197–200 (2005).
9. J. He, N. Kumar, M. Z. Bellus, H.-Y. Chiu, D. He, Y. Wang, H. Zhao, Electron transfer and coupling in graphene-tungsten disulfide van der Waals heterostructures. *Nat. Commun.* **5**, 5622 (2014).
10. N. Huo, Z. Wei, X. Meng, J. Kang, F. Wu, S.-S. Li, S.-H. Wie, J. Li, Interlayer coupling and optoelectronic properties of ultrathin two-dimensional heterostructures based on graphene, MoS_2 and WS_2 . *J. Mater. Chem. C* **3**, 5467–5473 (2015).
11. M. Massicotte, P. Schmidt, F. Violla, K. G. Schädlér, A. Reserbat-Plantey, K. Watanabe, T. Taniguchi, K. J. Tielrooij, F. H. L. Koppens, Picosecond photoresponse in van der Waals heterostructures. *Nat. Nanotechnol.* **11**, 42–46 (2016).
12. H. M. Hill, A. F. Rigosi, A. Raja, A. Chernikov, C. Roquelet, T. F. Heinz, Exciton broadening in WS_2 /graphene heterostructures. *Phys. Rev. B* **96**, 205401 (2017).
13. L. Yuan, T.-F. Chung, A. Kuc, Y. Wan, Y. Xu, Y. P. Chen, T. Heine, L. Huang, Photocarrier generation from interlayer charge-transfer transitions in WS_2 -graphene heterostructures. *Sci. Adv.* **4**, e1700324 (2018).
14. J. He, D. He, Y. Wang, H. Zhao, Probing effect of electric field on photocarrier transfer in graphene- WS_2 van der Waals heterostructures. *Opt. Expr.* **25**, 1949–1957 (2017).
15. Z. Song, H. Zhu, W. Shi, D. Sun, S. Ruan, Ultrafast charge transfer in graphene- WS_2 Van der Waals heterostructures. *Optik* **174**, 62–67 (2018).
16. A. Avsar, J. Y. Tan, T. Taychatanapat, J. Balakrishnan, G. K. W. Koon, Y. Yeo, J. Lahiri, A. Carvalho, A. S. Rodin, E. C. T. O'Farrell, G. Eda, A. H. Castro Neto, B. Özyilmaz, Spin-orbit proximity effect in graphene. *Nat. Commun.* **5**, 4875 (2014).
17. T. P. Kaloni, L. Kou, T. Frauenheim, U. Schwingenschlögl, Quantum spin Hall states in graphene interacting with WS_2 or WSe_2 . *Appl. Phys. Lett.* **105**, 233112 (2014).
18. T. Wakamura, F. Reale, P. Palczynski, S. Guéron, C. Mattevi, H. Bouchiat, Strong Anisotropic Spin-Orbit Interaction Induced in Graphene by Monolayer WS_2 . *Phys. Rev. Lett.* **120**, 106802 (2018).
19. A. Rossi, D. Spirito, F. Bianco, S. Forti, F. Fabbri, H. Büch, A. Tredicucci, R. Krahn, C. Coletti, Patterned tungsten disulfide/graphene heterostructures for efficient multifunctional optoelectronic devices. *Nanoscale* **10**, 4332–4338 (2018).
20. S. Omar, B. J. van Wees, Graphene- WS_2 -heterostructures for tunable spin injection and spin transport. *Phys. Rev. B* **95**, 081404(R) (2017).
21. A. Chernikov, T. C. Berkelbach, H. M. Hill, A. Rigosi, Y. Li, O. B. Aslan, D. R. Reichman, M. S. Hybertsen, T. F. Heinz, Exciton Binding Energy and Nonhydrogenic Rydberg Series in Monolayer WS_2 . *Phys. Rev. Lett.* **113**, 076802 (2014).
22. W. Yao, D. Xiao, Q. Niu, Valley-dependent optoelectronics from inversion symmetry breaking. *Phys. Rev. B* **77**, 235406 (2008).
23. D. Xiao, G.-B. Liu, W. Feng, X. Xu, W. Yao, Coupled Spin and Valley Physics in Monolayers of MoS_2 and Other Group-VI Dichalcogenides. *Phys. Rev. Lett.* **108**, 196802 (2012).
24. K. F. Mak, K. He, J. Shan, T. F. Heinz, Control of valley polarization in monolayer MoS_2 by optical helicity. *Nat. Nanotechnol.* **7**, 494–498 (2012).
25. H. Zeng, J. Dai, W. Yao, D. Xiao, X. Cui, Valley polarization in MoS_2 monolayers by optical pumping. *Nat. Nanotechnol.* **7**, 490–493 (2012).
26. V. Carozo, Y. Wang, K. Fujisawa, B. R. Carvalho, A. McCreary, S. Feng, Z. Lin, C. Zhou, N. Perea-López, A. L. Elias, B. Kabijs, V. H. Crespi, M. Terrones, Optical identification of sulfur vacancies: Bound excitons at the edges of monolayer tungsten disulfide. *Sci. Adv.* **3**, e1602813 (2017).
27. X. Hong, J. Kim, S.-F. Shi, Y. Zhang, C. Jin, Y. Sun, S. Tongay, J. Wu, Y. Zhang, F. Wang, Ultrafast charge transfer in atomically thin MoS_2/WS_2 heterostructures. *Nat. Nanotechnol.* **9**, 682–686 (2014).
28. F. Ceballos, M. Z. Bellus, H.-Y. Chiu, H. Zhao, Ultrafast Charge Separation and Indirect Exciton Formation in a MoS_2 - $MoSe_2$ van der Waals Heterostructure. *ACS Nano* **8**, 12717–12724 (2014).
29. P. Rivera, J. R. Schaibley, A. M. Jones, J. S. Ross, S. Wu, G. Aivazian, P. Klement, K. Seyler, G. Clark, N. J. Ghimire, J. Yan, D. G. Mandrus, W. Yao, X. Xu, Observation of long-lived interlayer excitons in monolayer $MoSe_2$ - WSe_2 heterostructures. *Nat. Commun.* **6**, 6242 (2015).
30. X. Zhu, N. R. Monahan, Z. Gong, H. Zhu, K. W. Williams, C. A. Nelson, Charge transfer excitons at van der Waals interfaces. *J. Am. Chem. Soc.* **137**, 8313–8320 (2015).
31. Y.-C. Lin, R. K. Ghosh, R. Addou, N. Lu, S. M. Eichfeld, H. Zhu, M.-Y. Li, X. Peng, M. J. Kim, L.-J. Li, R. M. Wallace, S. Datta, J. A. Robinson, Atomically thin resonant tunnel diodes built from synthetic van der Waals heterostructures. *Nat. Commun.* **6**, 7311 (2015).
32. H. Chen, X. Wen, J. Zhang, T. Wu, Y. Gong, X. Zhang, J. Yuan, C. Yi, J. Lou, P. M. Ajayan, W. Zhuang, G. Zhang, J. Zheng, Ultrafast formation of interlayer hot excitons in atomically thin MoS_2 - WS_2 heterostructures. *Nat. Commun.* **7**, 12512 (2016).
33. H. Wang, J. Bang, Y. Sun, L. Liang, D. West, V. Meunier, S. Zhang, The role of collective motion in the ultrafast charge transfer in van der Waals heterostructures. *Nat. Commun.* **7**, 11504 (2016).
34. Q. Zheng, W. A. Saidi, Y. Xie, Z. Lan, O. V. Prezhdo, H. Petek, J. Zhao, Phonon-assisted ultrafast charge transfer at van der Waals heterostructure interface. *Nano Lett.* **17**, 6435–6442 (2017).
35. Q. Zheng, Y. Xie, Z. Lan, O. V. Prezhdo, W. A. Saidi, J. Zhao, Phonon-coupled ultrafast interlayer charge oscillation at van der Waals heterostructure interfaces. *Phys. Rev. B* **97**, 205417 (2018).
36. K. V. Emtsev, A. Bostwick, K. Horn, J. Jobst, G. L. Kellogg, L. Ley, J. L. McChesney, T. Ohta, S. Reshanov, J. Röhrig, E. Rotenberg, A. K. Schmid, D. Waldmann, H. B. Weber, T. Seyller, Towards wafer-size graphene layers by atmospheric pressure graphitization of silicon carbide. *Nat. Mater.* **8**, 203–207 (2009).
37. K. V. Emtsev, F. Speck, T. Seyller, L. Ley, J. D. Riley, Interaction, growth, and ordering of epitaxial graphene on SiC(0001) surfaces: A comparative photoelectron spectroscopy study. *Phys. Rev. B* **77**, 155303 (2008).
38. C. Riedl, C. Coletti, T. Iwasaki, A. A. Zakharov, U. Starke, Quasi-free-standing epitaxial graphene on SiC obtained by hydrogen intercalation. *Phys. Rev. Lett.* **103**, 246804 (2009).
39. A. Rossi, H. Büch, C. Di Rienzo, V. Miseikis, D. Convertino, A. Al-Temimy, V. Voliani, M. Gemmi, V. Piazza, C. Coletti, Scalable synthesis of WS_2 on graphene and h-BN: An all-2D platform for light-matter transduction. *2D Mater.* **3**, 031013 (2016).
40. S. Forti, A. Rossi, H. Büch, T. Cavallucci, F. Bisio, A. Sala, T. O. Menteş, A. Locatelli, M. Magnozzi, M. Canepa, K. Müller, S. Link, U. Starke, V. Tozzini, C. Coletti, Electronic properties of single-layer tungsten disulfide on epitaxial graphene on silicon carbide. *Nanoscale* **9**, 16412–16419 (2017).

Acknowledgments

Funding: This work received financial support from the German Science Foundation via the Collaborative Research Centers 925 “Light induced dynamics and control of correlated quantum systems” (project B6) and 173 “Spin + X: spin in its collective environment” (project A02) and from the European Union’s Horizon 2020 research and innovation program under grant agreement nos. 696656 - GrapheneCore1 and 785219 - GrapheneCore2. **Author contributions:** A.R., S.F., C.C., and I.G. designed the original experiment. S.A., A.R., M.C.-C., R.K., and I.G. performed the tr-ARPES experiments. S.A., B.A., B.S., and M.A. obtained the high-resolution ARPES spectrum. A.R., S.F., and F.F. grew and characterized the samples. I.G. analyzed the data and wrote the manuscript with input from all coauthors. **Competing interests:** The authors declare that they have no other competing interests. **Data and materials availability:** All data needed to evaluate the conclusions in the paper are present in the paper and/or the Supplementary Materials. Additional data related to this paper may be requested from the authors.

Submitted 17 May 2019

Accepted 2 March 2020

Published 13 May 2020

10.1126/sciadv.aay0761

Citation: S. Aeschlimann, A. Rossi, M. Chávez-Cervantes, R. Krause, B. Arnoldi, B. Stadtmüller, M. Aeschlimann, S. Forti, F. Fabbri, C. Coletti, I. Gierz, Direct evidence for efficient ultrafast charge separation in epitaxial WS_2 /graphene heterostructures. *Sci. Adv.* **6**, eaay0761 (2020).